Solids Mixing and Circulation in Gas Fluidized Beds

ELIYAHU TALMOR and ROBERT F. BENENATI

Polytechnic Institute of Brooklyn, Brooklyn, New York

The circulation of solids in gas fluidized beds is known to be responsible for their unique characteristics. Yet, very few quantitative results have been published in the literature. The problem of different experimental conditions prevents a comparison among the published values for solids diffusion coefficients (*1, 2, 10, 12, 14*). Tailby and Cocquerel (*17, 18*) and Littman (*11*) report that their solids mixing data did not produce constant diffusion coefficients, while May (*14*) states that the presence of a gross circulation pattern makes his solids diffusion data erratic. Some mixing data are reported in terms of qualitative concepts (*17*) or partially reported in terms of arbitrarily defined mixing indices (*16*). Another recent study (9) considers the use of gas fluidization for blending two solids which differ in particle size and specific gravity.

Particle velocities were observed by high-speed photography of marked particles through a transparent bed wall (*13, 20, 21*) or of opaque traced particles by X-rays (*6*) and by timing the movement of traced particles from top to bottom of a bed (*7*). The latter is the only published work reporting bulk velocities of solids in gas fluidized beds. The three methods gave widely different results. According to Leva (*8*), the main reason for the disagreement is linked with particle shape. However, regardless of the different particles and bed diameters involved, the three methods could not be expected to have given the same results since the first measured a mean particle velocity at the bed wall, the second a similar mean at the interior of the bed, and the third a mean movement down through the whole bed. Microscopic and macroscopic treatments of fluidized beds cannot be expected to yield the same results. In this study the macroscopic approach was employed.

MODEL AND CHOICE OF EXPERIMENTAL CONDITIONS

Consider the two-region bed illustrated in Figure 1. The solids in both bed regions have the same density but may or may not have the same mean particle size provided that (D/D_p) is sufficiently high to avoid wall effects. Neglecting horizontal solids movement components, the variations of x and y with time are supposed to be established by a vertical up-and-down solids movement which is induced by the upward flow of air. In absence of wall effects, M_1 and M_2 will not vary with time; that is, upward and downward flows of solids will be equal.

A tracer balance for each one of the two bed sections will yield the following pair of differential equations (*4, 22*):

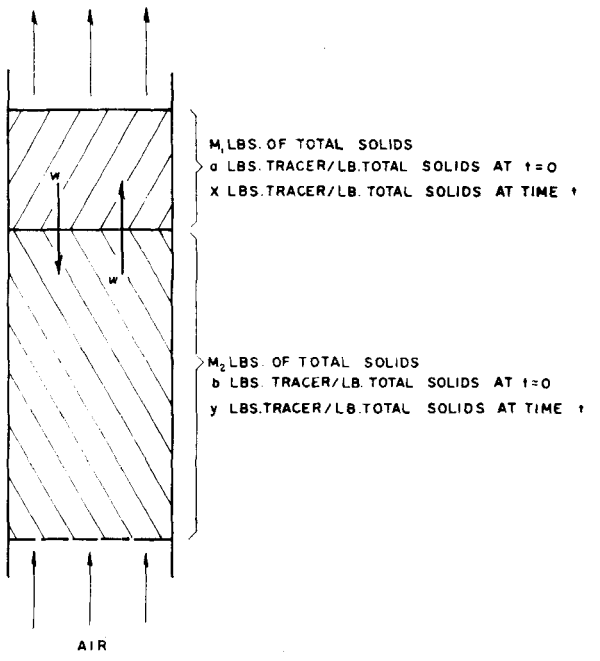

Fig. 1. Fluidized bed solids circulation model.

$$M_1 \frac{dx}{dt} = w(y - x) \tag{1}$$

$$M_2 \frac{dy}{dt} = w(x - y) \tag{2}$$

where w is defined as the macroscopic steady state solids circulation rate, mass per unit time, at any cross-sectional area of the bed. The initial conditions are

$$t = 0, x = a \tag{3}$$

$$t = 0, y = b \tag{4}$$

Simultaneous solution of Equations (1) and (2) yields

$$\ln \frac{a - b}{(1 + M_1/M_2)\, x - (M_1/M_2)\, a - b} = w\left(\frac{1}{M_1} + \frac{1}{M_2}\right) t \tag{5}$$

When the total initial tracer quantity equals the total solids in the upper section, that is

$$M_1 a + M_2 b - M_1 \tag{6}$$

Equation (5) takes the form

$$\ln \frac{1}{(1 + M_1/M_2)\, x - (M_1/M_2)}$$

The material presented in this paper is taken from the dissertation submitted to the faculty of the Polytechnic Institute of Brooklyn, New York, in partial fulfillment of the requirements for the degree of Doctor of Philosophy (chemical engineering) in 1962.

Dr. Talmor is at present with Rocketdyne, Canoga Park, California.

$$= w\left(\frac{1}{M_1} + \frac{1}{M_2}\right)t - \ln(a-b) \quad (7)$$

A similar equation can also be derived for y.

According to Equation (7), the logarithmic expression on its left-hand side is linear with $(1/M_1 + 1/M_2)t$ with a slope of linearity equal to w. Theoretically, only one observation of $(t; x)$ will determine w provided that the values of a and b are known. However, the prefluidization values of a and b may or may not correspond to the intercept of the straight line fit of the data in accordance with Equation (7). This depends on the rapidity of the transition to steady state solids circulation upon the introduction of air and, to a lesser degree, on the instantaneousness of the reaction of the operator with the stopwatch. Therefore, at least two observations of $(t; x)$ will be required to evaluate two unknowns in Equation (7): the slope w and the intercept $\ln(a - b)$. In any case several observations of $(t; x)$ at constant air flow rate should be made and w determined by a best straight line fit of the data in accordance with Equation (7).

When one solves for x and the equation is rearranged, x can be related to a dimensionless time variable, $wt/(M_1 + M_2)$, which is the fraction of bed turnover time (*19*). Curves of x vs. $wt/(M_1 + M_2)$ at constant values of (M_1/M_2) show clearly that the measurable ranges of x(or $x - x_{ss}$) decrease and their corresponding time ranges increase with increasing values of (M_1/M_2). Experimentation at either too low or too high values of (M_1/M_2) will make w very sensitive to the accuracy of $(t; x)$ observations. In between these extremes lies an optimum value of (M_1/M_2). The above-mentioned curves (*19*) indicate that the optimum range of experimentation will be at (M_1/M_2) of 0.1, or 10% tracer, and this tracer ratio was predominantly used in this study. Few data were taken with 20% tracer.

The model can also be used to investigate the relation, if any, between bed turnover and bed tracer uniformity (*19*). At bed turnover

$$w = (M_1 + M_2)/t \quad (8)$$

When Equation (8) is substituted into (7) and rearranged, it can be shown (*19*) that at bed turnover the approach to tracer uniformity, $(x - x_{ss})$, is a function of (M_1/M_2) only. For values of (M_1/M_2) up to and including 0.10, $(x - x_{ss})$ is zero for all practical purposes. For values of (M_1/M_2) higher than 0.10, the deviations of $(x - x_{ss})$ from zero become relatively appreciable. Leva and Grummer (*7*) assumed complete association between tracer uniformity and bed turnover. The foregoing discussion starting with Equation (8) could have given them a better justification for doing so at $(M_1/M_2) = 0.10$.

Zenz and Othmer (*22*) used an equation similar to Equation (7) to calculate values of w from the data of Leva and Grummer (*7*) and Koble (*5*). In the former case they assumed that Leva and Grummer's visual uniformity observations were quantitatively 99.9% of perfect mixing. In view of Equation (8), this assumption was not necessary. In the second case Zenz and Othmer (*22*) calculated w's from Koble's mixing data obtained after 15, 30, and 40 sec. of fluidization. It was not noticed however that Koble (*5*) used a continuous sampling technique; that is, the total bed weight $(M_1 + M_2)$ and the individual weights of tracer (M_1) and nontracer (M_2), all varied with time in a stepwise manner. In such a case Equation (7) can be used to calculate w's provided that the size of each sample is known, and thus the equation can be applied to any time interval between samples employing the bed weights (M_1 and M_2) existing during the time interval considered. Koble did not report his sample sizes. Therefore, Equation (7) can be applied to the first 15 sec. time interval only for which the initial bed weights of $M_1 = 1$ and $M_2 = 9$ are applicable.

In this study the data of Leva and Grummer (*7*) were reinterpreted by the use of Equation (8), and one possible value of w was calculated from the data of Koble (*5*) as outlined above. All these reinterpreted data were combined with newly obtained data for correlation purposes.

EXPERIMENTAL

Tracer Technique

The requirements initially set for the tracer were that it should have the same density and mean particle size as the untraced material and yet be readily analyzed when in mixtures with nontracer. The study was later extended to the use of tracer and nontracer of different mean particle sizes. However, the same particle density was maintained in both bed regions in all runs.

When tracer and nontracer had the same density and mean particle size, various techniques were considered (*19*). The one successfully used was the employment of oven-dry strongly acidic cation exchange resin, Dowex 50W X 8 in the hydrogen and sodium forms, heretofore designated as DH and DNa respectively. The spherically shaped solids were available in two nominal mesh classifications: 20 to 50 and 50 to 100. DNa was employed as tracer in beds of DH. Samples were chemically analyzed and remaining solids in the bed were regenerated for reuse.

When tracer and nontracer had different mean particle sizes, screening was the obvious analysis technique. Minus 40 United States mesh resin was used as tracer in beds of plus 40 United States mesh resin and vice versa.

Equipment

The basic flow diagram of the system used is shown in Figure 2. Column and bed support details are shown in Figure 3. The inside circumferential area of the sampling nozzles as well as the inner facings of the stoppers were all curved to the inside curvature of the tube to avoid any interference. The distribution plate was designed for 40% of the maximum anticipated bed pressure drop of 0.9 lb./sq. in., corresponding to a maximum anticipated bed height (before slugging) of 6 diam. (see below.)

Procedure

With each one of the two solids used, orienting runs were first made to determine the maximum possible bed height and to set the air flow rates to be used later during the actual mixing runs. It was found that slugging occurred at bed heights of 5.5 to 6 diam. A bed height of 5.5 diam. was chosen and used in all the 10% tracer mixing runs. The 20% tracer mixing data were taken with overall bed heights of 4.8 diam.

When tracer and nontracer had the same Dp with tracer located at the top of the bed, a typical run consisted of first charging the column with DH up to 5.5-diam. height. The blower was then started and the globe valve and/or plug valve positions were set to the desired air flow rate. The blower was then stopped and the upper portion of the bed (0.5 diam. high) withdrawn through and down to the top nozzle and replaced with the same quantity of DNa, the weights of both solids (M_2 and M_1) being recorded. Fluidization was now restarted and time measured by a stopwatch from the onset of fluidization to any desired duration. The run was terminated by a fast shutoff of the plug valve. No deaeration problems were encountered with the particle sizes involved. The bed was then sampled through each one of the top five nozzles starting from the top and proceeding down the column, removing through each nozzle all the solids above it. Six batches were thus obtained all ready for chemical analysis. Samples were withdrawn from each batch and their composition analyzed till all the tracer ($=M_1$) was accounted for. This resulted in a minimum of three analyses per batch.

When tracer and nontracer had different mean particle sizes with tracer located at either end of the bed, fluidization curves

had to be obtained for each tracer location and for each combination of particle sizes. The procedure, except for the analysis technique, was the same as previously described.

SOLIDS MIXING DATA

Three major categories of mixing data were taken:

1. Tracer and nontracer of same mean particle size with tracer located at the top of the bed (10 and 20% tracer).

2. Tracer and nontracer of same mean particle size with tracer located at the bottom of the bed (10 to 11% tracer).

3. Tracer and nontracer of different mean particle sizes with tracer located at either end of the bed (10 to 11% tracer).

For each particle size ($Dp_1 = Dp_2$) or combination of particle sizes ($Dp_1 \neq Dp_2$), the data consisted of run series with each series corresponding to an essentially constant air flow rate. Each run series was in turn composed of single mixing runs of different durations.

Figure 4 shows straight line fits of data in accordance with Equation (7). For complete data see reference *19**.

With $Dp_1 \neq Dp_2$, fluidization could not be achieved unless the air flow rate was higher than the minimum required to fluidize the larger particle size bed region. Even then, great difficulties were encountered in initiating fluidization whenever larger particles were present on top of smaller ones; that is, $Dp_1 > Dp_2$ with Dp_1 located at the top of the bed or $Dp_1 < Dp_2$ with Dp_1 located at the bottom of the bed. In the first case severe slugging occurred at the top of the bed and in the second case slugging occurred at the bottom of the bed with the entire bed, tracer and nontracer, both unmixed, rising up the column as a slug, 5.5 diam. high. In both cases mixing was finally achieved by tapping the column at the slugging region. In most cases tapping resulted in the downward drop of the slugging bed portion and the onset of fluidization. In other cases the downward drop of the slugs owing to tapping resulted in a stagnant bed. Fluidization could then be restarted by reslugging and tapping; however, repeated cycles of operation made such runs useless owing to the irreproducibility of the initial tracer conditions at $t = 0$.

SOLIDS CIRCULATION RATES, DATA, AND CORRELATION

The solids circulation rates, w, as calculated from the mixing data were in terms of mass per unit time. In all cases the calculated values of w were multiplied by 3,600 and divided by the cross-sectional area of the column involved to obtain values of W, lb./(hr.)(sq. ft.). Over the range of bed diameters studied, the presentation of the solids circulation rates on a superficial basis eliminated the parameter of bed diameter from the correlation that will be subsequently presented.

Correlation of solids circulation rates was first sought for the $Dp_1 = Dp_2$ data since in this case there was no question as to the mean particle size to be used. The resulting correlation made way for the interpretation of the $Dp_1 \neq Dp_2$ data.

It was found that for each mean particle size involved, the superficial solids circulation rate W was linear with the excess of superficial air flow rate over the minimum required for fluidization, or

$$W = m(G - G_{mf}) \tag{9}$$

where m, defined as $W/(G - G_{mf})$, was termed the solids circulation ratio. The solids circulation ratios were in turn found to vary exponentially with the mean particle size only, or

$$m = 654e^{-168.5\,Dp} \tag{10}$$

When Equations (9) and (10) are combined

$$W = 654\,[(G - G_{mf})\,e^{-168.5\,Dp}] \tag{11}$$

which is graphically shown in Figure 5. Rectangular coordinates could yield the same straight line shown in Figure 5, however, the log-log coordinates used indicate more clearly the range of data taken in this study with respect to the reinterpreted data from the literature.

Equation (11) or Figure 5, the finally obtained correlation of solids circulation rates in gas fluidized beds, covers the following range of variables:

Particle size	0.00264 to 0.0257 in.
Particle size distribution	mixed and uniform

* Microfilm or other copies are obtainable from University Microfilms, University of Michigan, Ann Arbor, Michigan.

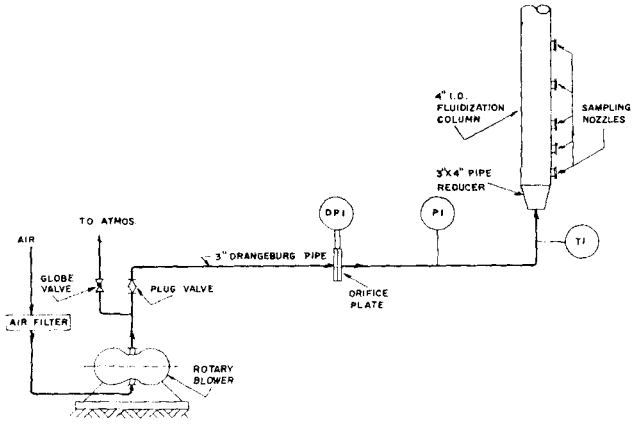

Fig. 2. Experimental unit.

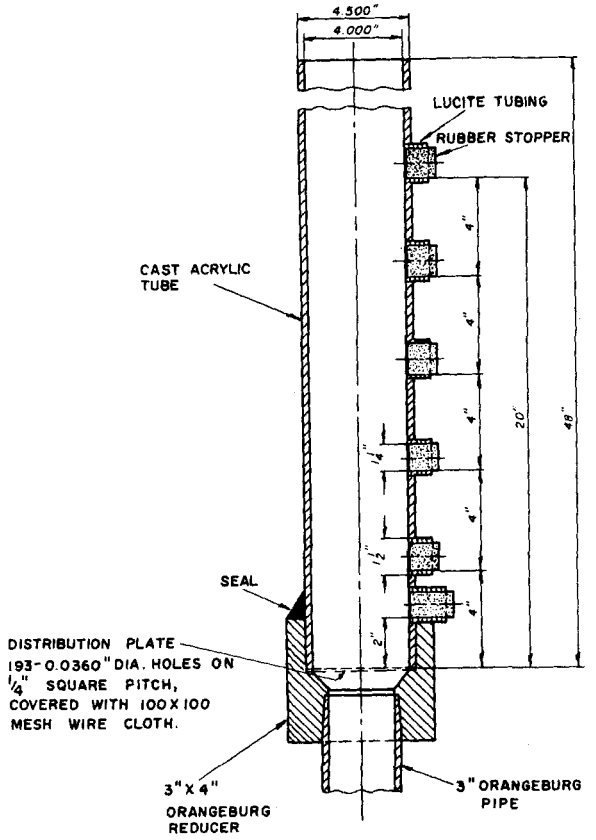

Fig. 3. Column and bed support details.

Particle density	75 to 165 lb./cu. ft.
Particle shape	granular to spherical
Bed diameter	1.32 to 4.00 in.
$(G - G_{mf})$	0 to 250 lb./(hr.)(sq. ft.)

The average standard deviation is 23%.

In the presentation of the solids circulation rates calculated from the $Dp_1 \neq Dp_2$ mixing data, the question arose as to which G_{mf} and Dp were to be used in the abscissa of Figure 5. The corresponding fluidization curves indicated that the G_{mf} value of the larger particles was the only one that could be logically used. Once this was established, the data points were plotted as W vs. $(G - G_{mf})$ and they were found to cluster the zone corresponding to the Dp of the smaller particles regardless of whether the smaller particles were used as a tracer or non-tracer; that is, the circulation ratio of the smaller particles was controlling. Thus, the G_{mf} of the larger particles and the Dp of the smaller particles were used respectively in the numerator and denominator of the abscissa of Figure 5 for presentation of the W's related to the $Dp_1 \neq Dp_2$ mixing data. The single point of Koble (5) is presented in the same manner.

DISCUSSION

The tracer gradients obtained did not render themselves to diffusional treatment. The diffusion concept could apply superficially when the tracer concentration of the initially traced region stays maximum at all times. However, in many cases the tracer concentration of some bed section of the initially untraced region passed through a maximum and this is the phenomenon that made May's diffusion data (14) erratic. The model used employs average bulk tracer contents for each one of the two bed regions involved. Yet, despite the presence of gradients,

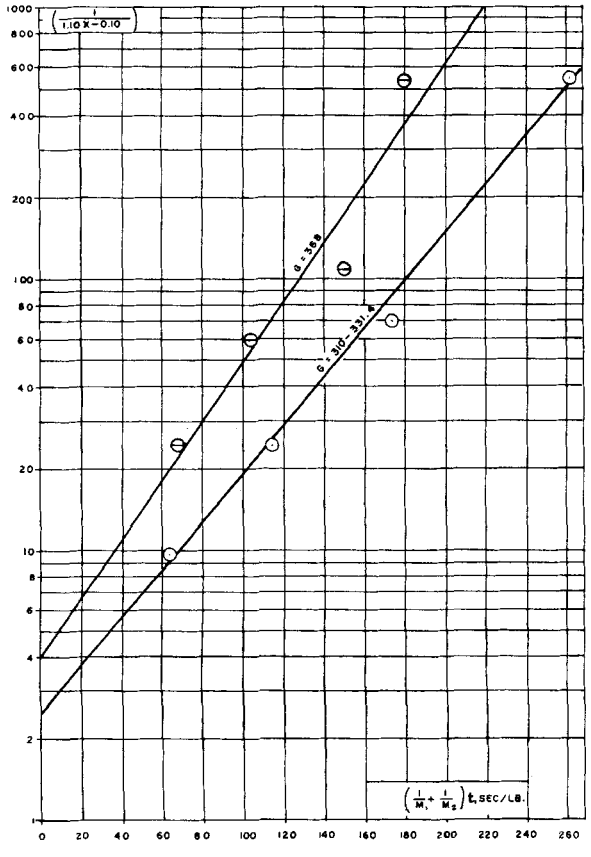

Fig. 4. The straight line fit of the data in accordance with Equation (7). G = 310-368 lb./hr./sq. ft., Pp_1 = Dp_2 = 0.0257 in. Tracer initially at the top of the bed.

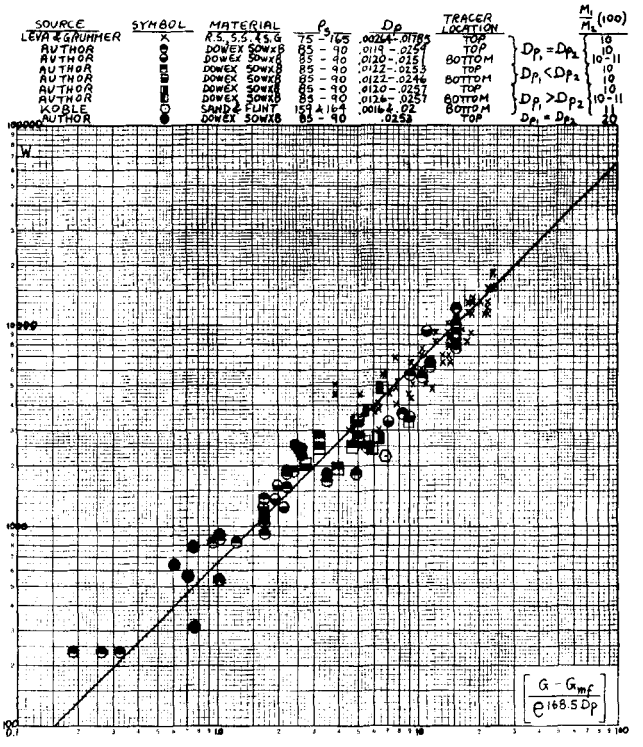

Fig. 5. Correlation of solids circulation rates in gas fluidized beds. Units: W, G, and Gmf — lb./(hr.)(sq. ft.); Dp — in.

the model holds; that is, the data follow the straight line fit suggested by the model. This is not a paradox. The solids flowing into any bed region are entrained from all the sections of the other region. Thus, the bed region in question senses a solids input with a tracer concentration close to the average of the entire other region. This average tracer concentration is identical to that obtained with complete mixing within the region. However, the assumption of perfect instantaneous mixing in each bed region is not necessary.

The sizes of the two regions undergoing mixing are fixed. There is a tracer concentration discontinuity at the boundary of the two bed regions at $t = 0$ and the mixing data show this discontinuity during the unsteady state mixing process too, that is, while the tracer content of the initially traced region (M_1) goes down with time, that of the initially untraced region (M_2) goes up with time. The model concerns itself with the solids transfer across the initial boundary between the two bed regions and this boundary corresponds to a given ratio of M_1 over M_2 throughout the mixing run. (M_1/M_2) and w are the model's two parameters while the diffusion model has only one parameter. Since one more parameter is used, better fit of the data is expected. However, only one parameter, W, correlates against the system variables and the improvement of the resulting correlation is reflected in the range of variables it covers.

The mutual agreement of the solids circulation rates obtained with tracer located at either end of the bed is of major significance. The literature reports the presence of inactive bottom bed portions and this was directly related to the gas distributor design (3). From the standpoint of the superficial mass solids circulation rate, no performance deficiencies were encountered with the distribution device described in Figure 3. It may now be concluded that solids mass circulation rates in gas fluidized beds are not affected by the gas distributor as long as the latter is properly designed for effective gas distribution (for example, 40% of bed pressure drop).

The solids circulation rates presented in this study do not apply to channeling or slugging beds, nor do they apply to any performance deficiencies resulting from improperly designed distributors. The latter, to the degree that they are present, affect the expansion behavior of the bed (3). But bed expansion does not affect the superficial mass circulation rate of the solids. It is, however, of major importance when bulk linear velocities are sought, such as were calculated by Leva and Grummer (7). The superficial mass circulation rate can be considered as the product of the solids bulk linear velocity and the bulk density of the bed, or

$$W = u_s \rho_b \tag{12}$$

When one solves for u_s and substitutes for ρ_b

$$u_s = \frac{W}{\rho_s(1 - \epsilon)} \tag{13}$$

where ϵ is a function of several variables other than Dp, such as particle shape, particle size distribution, and gas distributor design. According to Equation (13), two beds, or two regions within a bed, having the same W may not have the same u_s, the latter being a function of solids density and local voidage, or any variables affecting voidage. The advantage of the mass circulation concept is thus obvious.

The extension of this study to larger beds is highly recommended. Solids circulation and mixing in gas fluidized beds are essentially caused by gas bubbles moving through the bed (*15*). This is well reflected by the fact that $(G - G_{mf})$ is one of the two factors affecting W. It is well known by observations that when fluidizing with gas, all the fluid in excess of that required for incipient fluidization passes through the bed as bubbles. This direct relationship between solids circulation and gas bubbles complicates the applicability of the results of this study to larger size equipment.

The foregoing discussion does not take anything away from the value of the results obtained thus far. The correlation presented constitutes an agreement of data from different sources and this is the first time that such an agreement has been obtained.

CONCLUSIONS

1. The factors affecting the superficial mass solids circulation rates in gas fluidized beds are the mean particle size and the excess of superficial mass gas flow rate over the minimum required for fluidization.

2. For any given mean particle size, the superficial mass solids circulation rate is linearly proportional to the excess of superficial mass gas flow rate over that required for incipient fluidization with slopes of linearity, termed circulation ratios, which are a function of the mean particle size only.

3. The solids circulation ratios in gas fluidized beds vary exponentially with the mean particle size.

ACKNOWLEDGMENT

The authors wish to acknowledge the assistance of Mrs. E. Talmor, Dr. F. A. Zenz, and Mr. R. Moroz.

Special thanks are due to the Dow Chemical Company, Midland, Michigan, for supplying the resins for this study.

NOTATION

- a = tracer weight fraction of an originally traced bed region at $t = 0$
- b = tracer weight fraction of an originally untraced bed region at $t = 0$
- D = bed internal diameter, in.
- Dp = mean particle size, in.
- Dp_1 = mean particle size of an originally traced bed region, in.
- Dp_2 = mean particle size of an originally untraced bed region, in.
- e = base of natural logarithms
- G = superficial mass air flow rate, lb./(hr.) (sq. ft.)
- G_{mf} = minimum superficial mass air flow rate required for fluidization, lb./(hr.) (sq. ft.)
- M_1 = weight of an initially traced bed region, lb.
- M_2 = weight of an initially untraced bed region, lb.
- m = solids circulation ratio in gas fluidized beds = $W/(G - G_{mf})$, dimensionless
- t = elapsed time, sec.
- u_s = solids bulk linear velocity, ft./hr.
- W = superficial mass solids circulation rate in gas fluidized beds, lb./(hr.) (sq. ft.)
- w = mass solids circulation in gas fluidized beds, lb./sec.
- x = tracer weight fraction of an originally traced bed region at any given time t
- x_{ss} = steady state tracer weight fraction of the bed = $M_1/(M_1 + M_2)$
- y = tracer weight fraction of an originally untraced bed region at any given time t
- ϵ = fractional bed voidage
- ρ_b = bulk bed density = $\rho_s(1 - \epsilon)$, lb./cu. ft.
- ρ_s = true solids density, lb./cu. ft.

LITERATURE CITED

1. Bart, Roger, Sc.D. thesis, Mass. Inst. Technol., Cambridge, Mass. (1950).
2. Brotz, Walter, *Chem.-Ing.-Tech.*, **28**, 165 (1956).
3. Grohse, E. W., *A.I.Ch.E. Journal*, **1**, 358 (1955).
4. Katz, S., and F. A. Zenz, *Petrol. Refiner*, **33**, No. 5. p. 203 (1954).
5. Koble, R. A., Ph.D. thesis, Univ. West Virginia, Morgantown, West Virginia (1952).
6. Le Bouffant, L., *Journee de Fluidisation*, **47** (1956).
7. Leva, Max, and Milton Grummer, *Chem. Eng. Progr.*, **48**, No. 6, p. 307 (1952).
8. Leva, Max, "Fluidization," p. 276, McGraw-Hill, New York (1959).
9. ———, Doctor of Eng. thesis, Tokyo Inst. of Technol., Tokyo, Japan (1961); *Third Congress of the European Federation of Chem. Eng.*, **B**, 30 (1962).
10. Levey, R. P., et al., *Report No. Y-1233*, Union Carbide Nuclear Company, Oak Ridge, Tennessee (1958); *Chem. Eng. Progr.*, **56**, No. 3, p. 43 (1960).
11. Littman, Howard, Paper presented at A.I.Ch.E. meeting in Baltimore, Maryland (May, 1962).
12. Massimilla, Leopoldo, and Sergio Bracale, *Ricerca Sci.*, **27**, 1509 (1957).
13. ———, and J. W. Westwater, *A.I.Ch.E. Journal*, **6**, 134 (1960).
14. May, W. G., *Chem. Eng. Progr.*, **55**, No. 12, p. 49 (1959).
15. Rowe, P. N., *Chem. Eng. Progr. Symposium Ser. No. 38*, **58**, 42 (1962).
16. Sutherland, K. S., *Trans. Inst. Chem. Engrs.*, **39**, 188 (1961).
17. Tailby, S. R., and M. A. T. Cocquerel, *Trans. Inst. Chem. Engrs.*, **39**, 195 (1961).
18. *Ibid.*, p. 237.
19. Talmor, Eliyahu, Ph.D. (Ch.E.) dissertation, Polytech. Inst., Brooklyn, New York (1962).
20. Toomey, R. D., and H. F. Johnstone, *Chem. Eng. Progr.*, **48**, No. 5, p. 220 (1952).
21. ———, *Chem. Eng. Progr. Symposium Ser. No. 5*, **49**, 51 (1953).
22. Zenz, F. A., and D. F. Othmer, "Fluidization and Fluid-Particle Systems," pp. 290-298, Reinhold, New York (1960).

Manuscript received July 18, 1962; revision received February 13, 1963; manuscript accepted February 14, 1963.